Project Acronym:

MRBREASTBIO (CONCEPT/0521/0040)

MRI breast robotic system for biopsy

Deliverable number: 3.1

Title: Two DOF robotic system

Prepared by:

Marinos Giannakou (MEDSONIC)
Anastasia Antoniou (CUT)
Christakis Damianou (CUT)

Date: 25/10/2022

Co-funded by the European Union

Republic of Cyprus

RESEARCH & INNOVATION FOUNDATION

Contents

Executive summary

The MRBREASTBIO robot is a 2 Degrees of Freedom (DOF) positioning device which performs a breast biopsy procedure under MRI guidance. The developed device is an MR compatible robotic system consisted of two individual motion stages. These stages navigate a needle supporter, inside which a biopsy needle is passed, to target a breast tumor.

One of the individual motion stages is the X-stage which produces the desired horizontal motion (along the x-axis). The Y-stage is the second individual stage of motion that generates the desired vertical displacement of the needle supporter (y-axis).

The entire positioning device has been developed by using MR compatible construction materials. Motors and encoders that are used to achieve the accurate motion of the biopsy system.

Introduction

Breast cancer is the most common form of cancer malignancy in women and the fifth cause of cancer-related death worldwide [1]-[2]. Diagnosis at an early stage provides patients with the best management and increased survival rates. Following clinical examination and imaging assessment, percutaneous biopsy is required for lesions suspicious for malignancy. A 30-40 % of performed biopsies are open surgical biopsies [3]. Percutaneous needle biopsies constitute an alternative to surgical biopsies, and they are usually guided by ultrasound (US), mammography or magnetic resonance imaging (MRI). They are faster, less invasive, and less expensive than surgical biopsy while offering analogous accuracy with less complications.

US is the modality of choice for image-guided biopsy of soft lesions that are visible on US and is usually performed free-handed using core biopsy (CB) sampling. It provides real-time guidance, without ionizing radiation as well as accessibility to all breast areas [4], [5]. However, it requires skilled personnel since the doctor performs the procedure while holding the transducer in one hand and the biopsy needle in the other. Accordingly, it has been reported that doctors usually suffer from fatigue and various musculoskeletal problems [6]. Accordingly, various robotic systems for US-based needle guidance have been developed on experimental level through the years to address these limitations. Most of them are based on the same principle, where the doctor marks the region of interest on the acquired US image, and its corresponding coordinates are registered on the robotic system, which then moves to align the needle with the desired location for final insertion by the doctor [7].

Around two decades ago, an US-guided biopsy system featuring eight degrees of freedom (DOF) had been proposed by Megali et al. [8]. Later, Mallapragada et al. [9], [10] followed a different approach and developed a robotic system for manipulating the breast mass instead of the needle. Around the same time, a 2D US-guided robotic arm comprising a 14G needle was developed and found to possess a trajectory error of 0.75 mm, thus being suitable for targeting lesions smaller than 2 cm in diameter. The system was tested by radiologists on chicken tissue and was found to be faster and more accurate than the free-hand technique [11]. A novel robotic system was also developed by Smith et. al. [12] for CB under 3D US guidance simultaneously offering breast stabilization. The system was proven able to position a 14G needle with a 1.16 mm accuracy in the XY plane and a 0.85 mm accuracy in the YZ plane [12]. Notably, Nelson et al. [13] presented a complete biopsy system featuring a six-DOF robotic arm and a dedicated table for prone positioning of the patient. The accuracy of the system was tested and found to be within 1 mm. Later, a five-DOF system with an estimated mean positioning error of 1.29 mm was developed for curved tissue surfaces, featuring a torque detector for adjusting the force exerted by the probe [14]. More recently, a mechanical end-effector for 3D US guided biopsy that can accommodate needles of any size has been proposed [15]. It offers needle guidance in three DOF while needle insertion is performed by the user and was found to have a 0.3 mm accuracy, thus making it possible to target lesions between 4-10 mm [15].

Stereotactic mammography guidance is usually the gold standard for tumors that are not visible on US images such as microcalcifications. It can be performed on a biopsy table with the patient in the prone position, or as an add-on unit on the existing mammographic equipment [16]. In either techniques, the breast is compressed and vacuum assisted biopsy (VAB) sampling is usually preferred due to the smaller rates of false-negative results [3]. There are several commercially available robotic mechanisms for needle alignment under stereotactic mammography guidance. As an example, the Affirm biopsy system from the American company Hologic (California, USA) exists both as an add-on unit [17] and a table system [18]. They are both based on mammographic images, on which the doctor marks the region of interest. The needle holder is then automatically moved to the corresponding coordinates in the XY plane (with 1 mm target accuracy) for manual insertion of the needle in the Z direction. Interestingly, a few mechanical systems have been developed on a research level combining both US and stereotactic mammography guidance to overcome the limitations each modality presents when used as a stand-alone method [19]–[21].

MRI is increasingly being used as a guidance modality for breast biopsy, especially for women with a high risk of breast cancer [22]. Since small lesions may not be detectable with the standard methods [23], an MR-guided biopsy is needed to histologically determine possible malignancy of the tumor. VAB is usually the sampling method of choice since various studies have proven that it is advantageous over the other methods in terms of successful tissue acquisition and accuracy [24], [25]. The patient is commonly in a prone position on a specially designed MR bed with a hole for the breasts, which are immobilized by vertical compression plates for avoiding any shift during the procedure [26]. An initial scanning is conducted for lesion localization. The optimum hole of a localization grid (lying in line with the lesion), as well as the insertion depth of the needle are determined by a combined biopsy software [26]. Then, the patient is moved out of the bore and a sheath is inserted, through which the biopsy needle will be advanced to the target. The coaxial sheath is placed with the help of a stylet, which is replaced by a plastic MRI-visible obturator. An additional scan is followed to confirm that the obturator's location coincides with that of the target [26]. The biopsy is usually performed outside of the magnet and involves inserting a hollow needle towards the lesion. Lateral approach of the needle is recommended [27], especially for deep lesions [28], with the localization methods involving grid, pillar and post, as well as free-hands techniques [29].

Even though high successful rates of the current approach of MR-guided breast biopsy have been achieved in several studies, the technique presents several limitations, including the requirement to move the patient in and out of the scanner multiple times, the possible lesion movement due to involuntary movements or tissue-needle interaction, the pointless acquisition of large volume of tissue and the long-term procedures [30]. Therefore, a robotic contribution in the overall procedure would definitely be essential for addressing the aforesaid limitations, thus providing a more accurate and efficient biopsy of the involved lesions.

Some initial trials for robotic interventions in the breast in the MRI setting resulted in the development of a six-DOF robotic system for both biopsy and therapy of breast tumours [31], a system for remote intervention in the breast controlled by means of ultrasonic motors [32] and a single DOF teleoperated needle driver robot [33]. Later, a six-DOF master-slave robotic system intended to be placed underneath the headrest was developed [34] for accurate needle positioning and insertion. Actuated by five pneumatic cylinders and one piezo motor, the slave robot can be tracked in the MRI coordinates, allowing the physician to operate the master console under real-time MRI guidance. The robot utilizes a 12G high field MRI coaxial needle with a diamond-shaped tip. Although sufficient target accuracy was achieved, the robot workspace is confined, and access to challenging lesion locations is infeasible [34]. A six-DOF Image-guided Automated Robot (IGAR) actuated by piezoelectric motors was also designed to be accommodated under the headrest [35]. Needle interventions were performed only outside of the MRI bore utilizing an introducer-localization system and a sub-millimeter targeting ability in free space was estimated [35].

More recently, a piezoelectrically actuated robotic manipulation system (MR-SON) with four DOF controlled by an image guidance software was manufactured [36]. Its slim design makes it suitable for lateral approach of the needle since it can be fitted on the MRI bed between the patient and the gantry. Due to confined workspace, a bendable 13-G needle was used instead. Although a lateral approach is advantageous for targeting challenging lesions, the insertion of the bendable needle is limited only in several directions. Additionally, since real-time tracking of the needle is not available, an MR marker block is utilized for that purpose. Experiments performed in a breast phantom showed a targeting accuracy of ± 2.5 mm [36].

More technological advances have seen the production of the “Stormram 4”, which is a four-DOF serial kinematic manipulator driven by two liner and two curved pneumatic stepper motors [37]. It constitutes a 3D printed improved version of earlier designs [38],[39], in terms of accuracy, size, complexity, and provided workspace. It utilizes curved air-pressure motors allowing it to fit inside the MRI scanner and operate while the magnet is in function. Lateral approaches for automatic insertion of the needle are allowed. According to trials in breast phantoms, this robot offers needle targeting with a mean positioning error of 1.29 ± 0.59 mm.

It is interesting that a novel palm-shaped breast deformation robot was designed [40] to be placed in the MR bore, aiming to optimize breast compression and provide flexible breast configuration and comfort to the patients. With multiple DOF actuated by a piezoelectric motor and multiple pneumatic bladders, the robot can compress the breast in multiple angles, thus increasing the biopsy precision [40].

Although the previously described systems can be utilized in combination with an MRI device, they have several limitations compared to the proposed one. Herein, the developed device was specially designed for particular application in the biopsy of breast tumours and is characterized by a simplified design with all the mechanical components arranged compactly in a rectangular frame behind the biopsy grid. It can be placed laterally to the patient (between the patient and the gantry) providing lateral approach of the needle, which is beneficial especially for deep lesions while leaving sufficient space for comfortable placement of the patient, given its compact and slim design. This configuration also enhances the safety of the procedure since there are no moving (mechatronic) parts at the side of the patient. The aforementioned systems are more complex in design and operation and in some cases the biopsy device is positioned underneath the patient, thus requiring modification of the MRI table or the addition of a dedicated table. On the contrary, the one proposed herein is universal and can be seated on the table of any conventional scanner of up to 7T magnetic field. It is portable due to its small size and light weight. It is also straightforward to use and cheaper in production and maintenance because of its cost-effective and simple design. Furthermore, by manual insertion of the needle by the physician the factor of “human control” is maintained.

Results

Figure 1 shows the robotic system that has been developed to be used as a positioning device that moves a biopsy needle in order to complete a breast biopsy procedure. The robotic system is constructed by MR-compatible materials and components and has been designed to be able to be used in MRI scanners. The Inventor Software® has been used to design the entire robotic system and a 3D printer (F270, Stratasys, Minnesota, USA) to produce its individual parts. The robotic system is constructed by Acrylonitrile Butadiene Styrene (ASA) plastic and Polylactic acid (PLA) plastic.

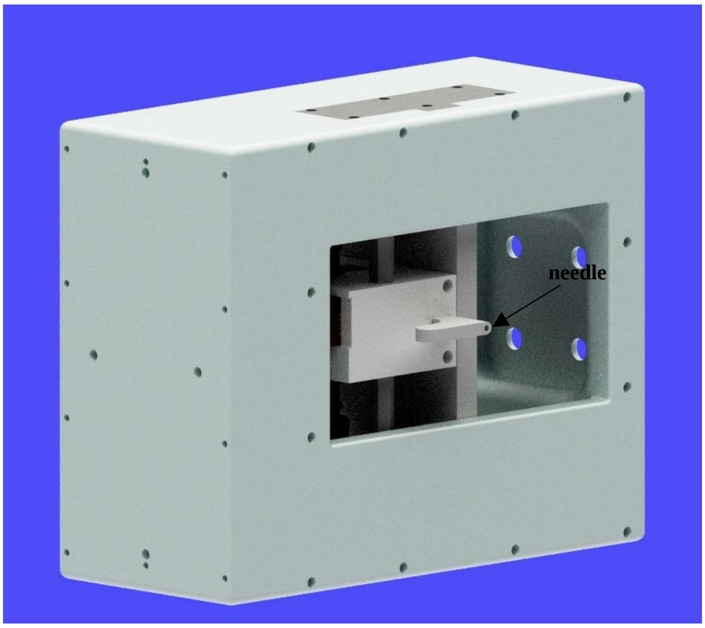

Figure 1: Robotic system: MRBREASTBIO

The current robotic positioning device is consisted of two positioning systems; the X-stage and Y-stage that aim to produce the desired motion. The combination of the abovementioned stages of motion accommodates a biopsy needle to be moved in 2 cartesian axes. Two MR compatible motors (USR60-S3N, Shinsei Kogyo Corp., Tokyo, Japan) are used to individually provide to the X-stage and Y-stage the desired motion. Additionally, the detection of the biopsy needle's position and the accuracy of its position's accuracy are important to be achieved. Thus, two MR compatible Optical encoders (EM1-0-500-I, US Digital Corporation, Vancouver, Washington, USA) that monitor the displacement of both X-stage and Y-stage were incorporated. The signals that the chosen non-magnetic motors and encoders produce do not interference with the MRI scanner signals. Except for this, the motors are non-magnetic motors. The needle supporter, illustrated in Figure 2, is used to create the path through which the biopsy needle passes.

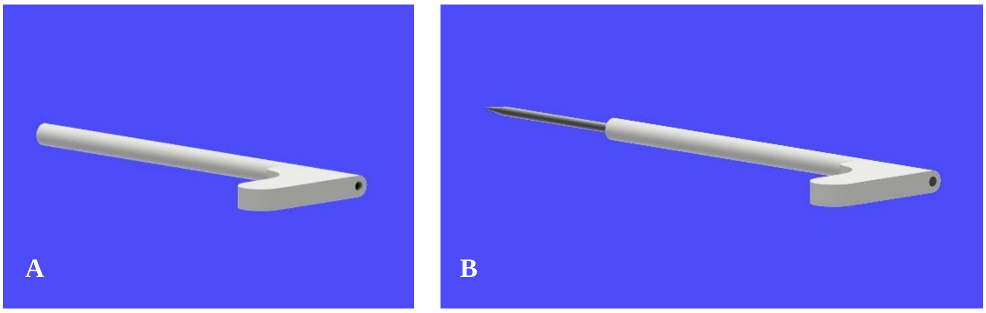

Figure 2: (A) Needle support (B) Needle support with biopsy needle

The Figure 3 shows the robotic system's parts that contribute to the production of the Y-stage motion. The Y-motor and the components that have been designed to generate the Y-stage motion (horizontal motion) are shown in Figure 3A. These components are the driver brace, the thread, the jack screw and two polygonal shaped drive shafts. The driver brace includes the three spaces to which a syringe and the needle supporter are inserted. The implementation of these spaces increases the range of motion of the Y-stage. In other words, the upper and lower spaces give the capability to the user (doctor) to target breast tumours that are located at the upper and lower ends of the Y-stage.

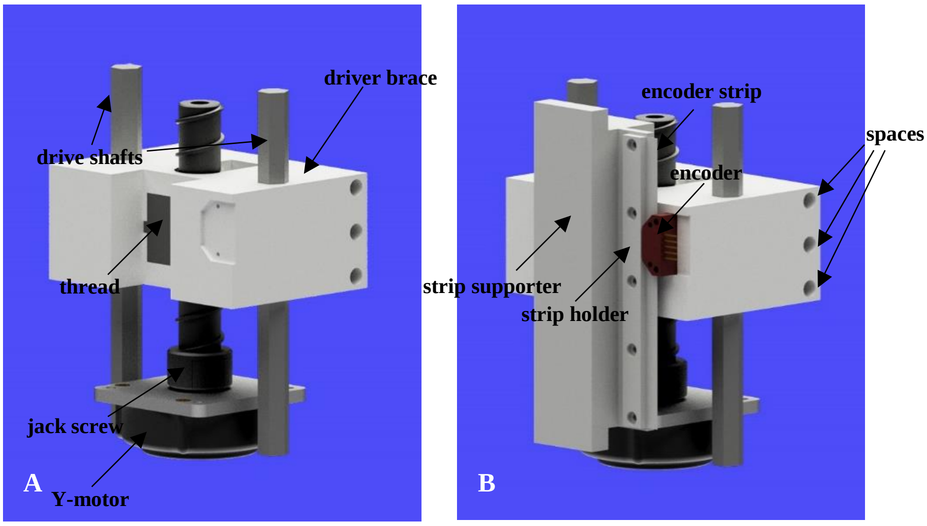

Figure 3: (A) Y-stage motion part (B) Y-stage motion part with encoder system

The vertical motion of the driver brace is provided by the jack screw's rotation. Specifically, the Y-motor to which the jack screw is coupled, force the jack screw to rotate inside the thread which is rigidly located in the driver brace's side surface. The thread is constructed with thread cutting, as it is shown in Figure 4. The described thread cutting has been developed to create the path inside which the jack screw's thread rotates. As a result of this, the jack screw's rotational motion is converted to the thread's linear motion. Thus, the rigid connection between the driver brace and the thread leads to the linear motion of the driver brace.

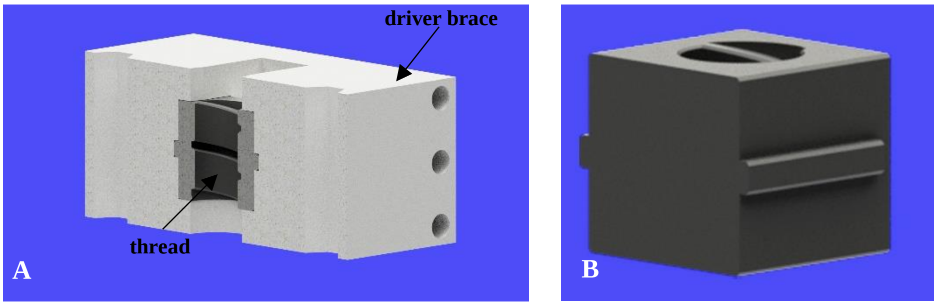

Figure 4: (A) Section view: Driver brace with Thread (B) Thread

Two polygonal shaped drive shafts that are shown in Figure 5A, have been inserted to ensure the stability of the driver brace throughout its vertical movement. The drive shafts are constructed considering the unhindered vertical motion of the driver brace that must be occur. Another function of the drive shafts is to provide to the needle supporter the motion that the X-stage of the robotic system produces. This becomes feasible due to the interconnection between the two driver braces of the X-stage and the driver brace of the Y-stage that is achieved due to the insertion of the drive shafts as it is shown in Figure 5B. The Figure 5B displays the interconnection between the three driver braces, while the Figure 5C shows the way the vertical drive shafts penetrate them. Inside the empty space that has been developed between each vertical drive shaft and the driver brace, a quantity of grease is used. The grease will be used to decrease the friction between the driver brace and the drive shafts, so that the desired movement occurs almost frictionlessly.

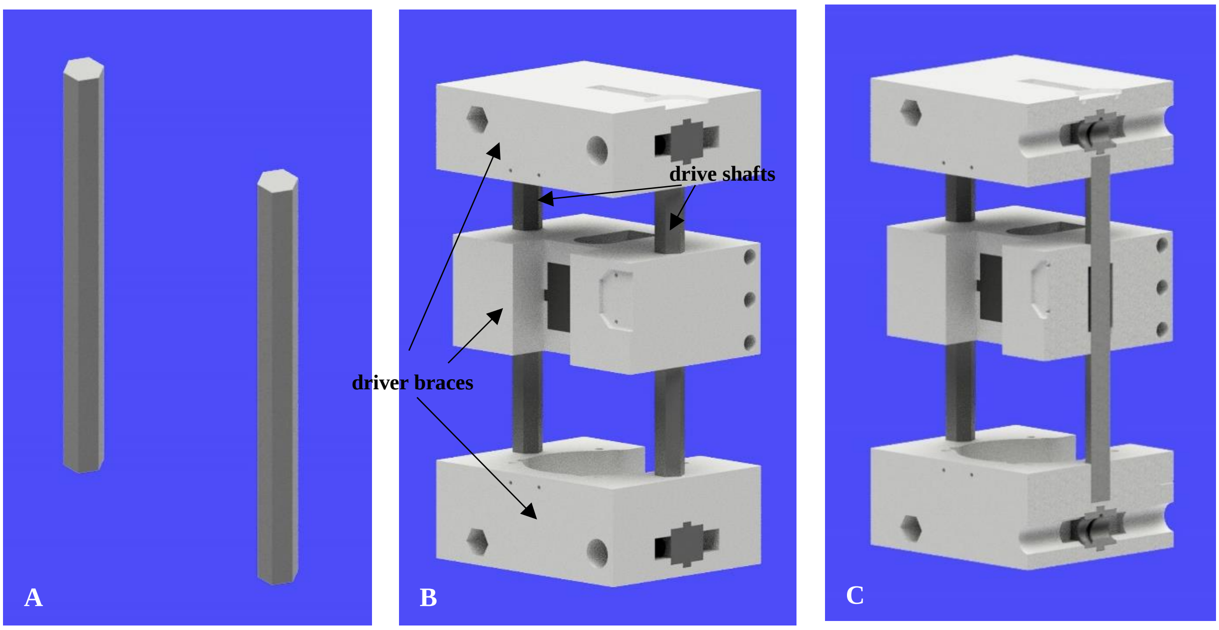

Figure 5: (A) Drive shafts (B) Interconnection of driver braces (C) Section View of B

A Y-stage encoder system, which is presented in Figure 3B, is inserted to detect and provide the accurate position of a biopsy needle along the Y axis. The Y-stage encoder system includes the encoder fixed on the driver brace, the encoder strip (LIN-500-5.5-1, US Digital Corporation, Vancouver, Washington, USA), the strip holder and the strip supporter. As the driver brace moves, the encoder follows the same vertical displacement along the encoder strip to detect the desired displacement. To achieve an accurate motion detection, the encoder strip must be rigidly placed. For this, the strip supporter and the strip holder are inserted to secure the encoder strip. The strip supporter, as it is shown in Figure 6, is hinged on the X-stage's driver braces to ensure its vertical orientation and to enhance the encoder strip's vertical stability.

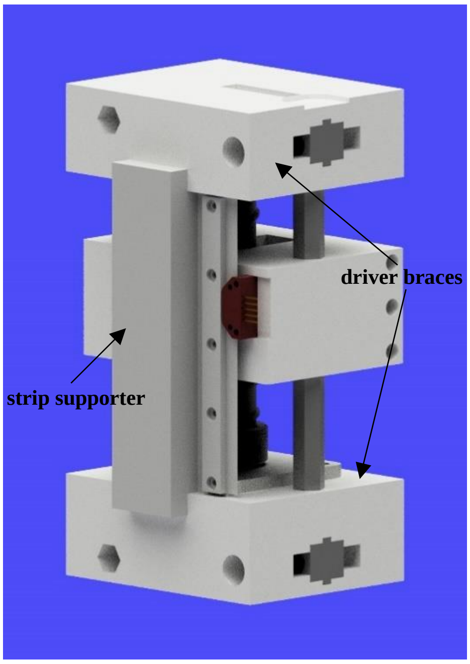

Figure 6: Y-stage motion with driver braces and Y-stage encoder system

The X-stage motion of the constructed robotic system is illustrated in Figure 7. The main parts that constitute the X-stage movement are the X-motor, the five gears, the two jack screws and the already mentioned driver braces. The X-motion is divided in two similar motions; the upper X-stage motion part and the lower X-stage motion part. The upper X-stage motion part includes the two gears that are located higher than the X-motor, the jack screw and the driver brace placed over the Y-stage's brace. The lower part consists of the two gears that are positioned below the X-motor, the jack screw and the driver brace that are installed under the Y-stage's driver brace.

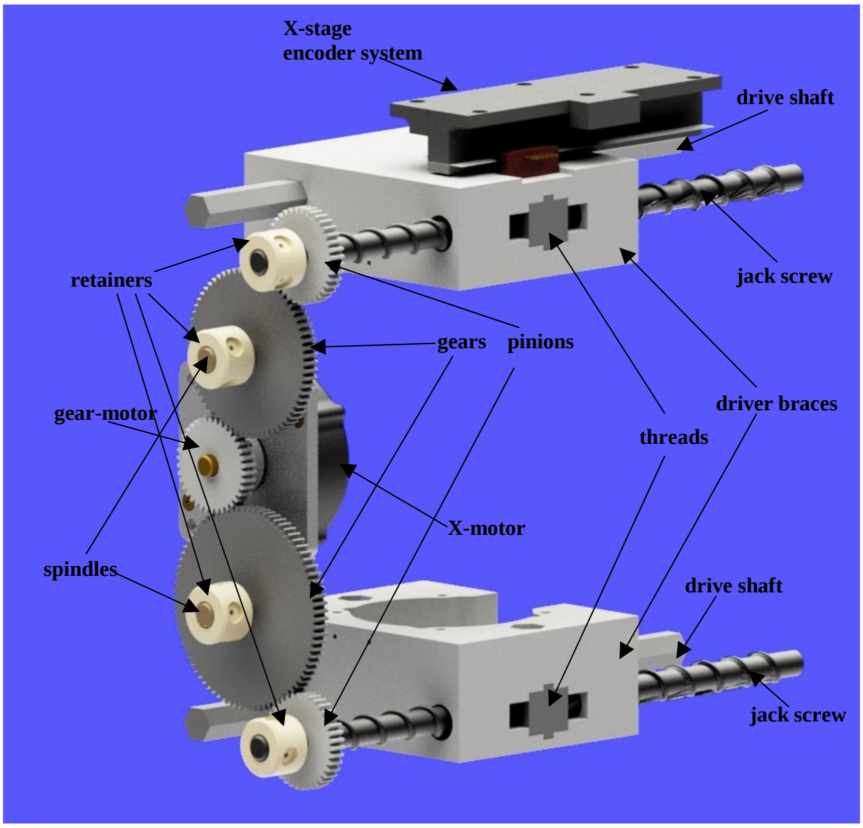

Figure 7: X-stage motion part

The production of the X-stage motion is based on the coupling between the motor and the gear-motor and on the way the gears of the upper and lower X-stage motion parts are interconnected. In more details, as shown in Figure 8, the gear-motor is tangentially connected to the gears that are tangentially connected to the pinions, respectively. The result of the abovementioned interconnections is the motion transfer, that occurs simultaneously, from the gear-motor to the two pinions that are placed at the ends of the gear system. These three gears have the same size; thus, their rotation speed and direction are equal.

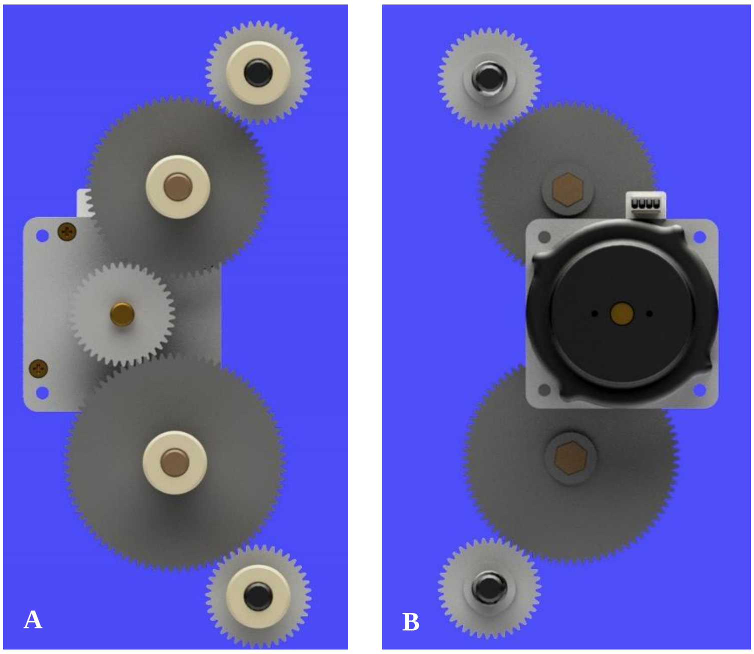

Figure 8: X-stage's Gear system with X-motor (A) Front side (B) Back side

Moreover, each of the pinions are coupled to the respective jack screws. Pinions' rotation led to the jack screws' simultaneous and equal rotation, as well. The driver braces establish the motion along the X-axis. Two threads are rigidly located to the driver braces. Each of the jack screws penetrate the respective thread to force the respective driver brace to move linearly along the X-axis. Similar to the Y-stage motion's thread, both of the threads are constructed with a thread cutting (Figure 9) on their inner surface through which the jack screw pass to convert its rotational motion into linear motion.

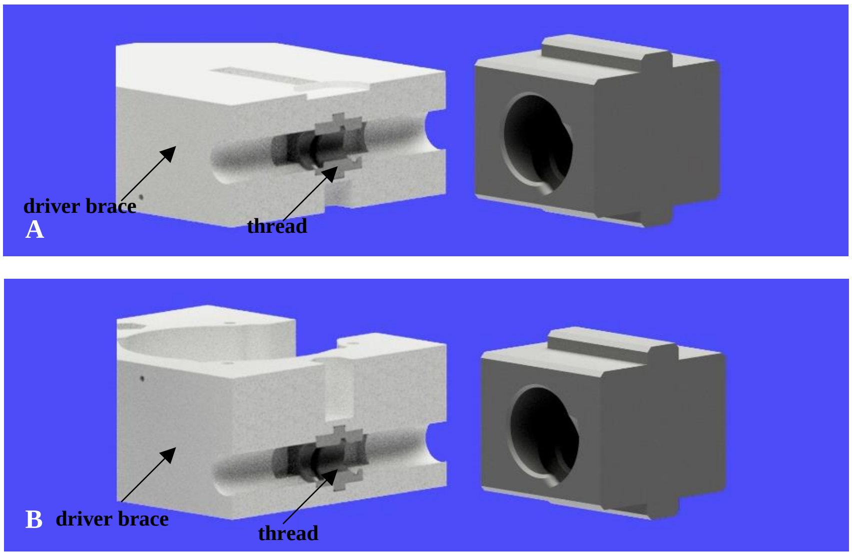

Figure 9: (A)Section view: Driver brace with Thread, Thread (B)Section view: Driver brace with Thread, Thread

Except for the jack screws, the drive shafts also penetrate the X-stage's driver braces. Specifically, both of the driver braces have been constructed with a polygonal shell similar to the shaped of the drive shafts. Through those shells the drive shafts pass to allow the driver braces' linear movement and to ensure that each of the driver brace keeps its orientation throughout the entire motion.

The Figure 10 shows the section view of both the driver braces and the way the drive shafts pass through them. The developed empty gap is used in the same way as the one that the Y-stage's driver brace has. Figure 11 shows, both drive shafts of the X-stage that are connected to the frame. The frame's main function is to enclose the mechanical components of the robotic system, as it is explained later. However, the rigid connection between the ends of each of the drive shafts and the frame, secure the drive shafts' position and stability. As a result of these connections, the stability of the entire X-stage's movable part is enhanced.

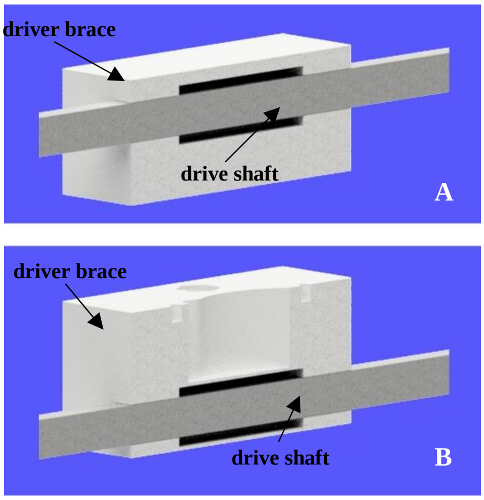

Figure 10: (A)Section view: Driver brace with Drive shaft of the upper X-stage (B)Section view: Driver brace with Drive shaft of the lower X-stage

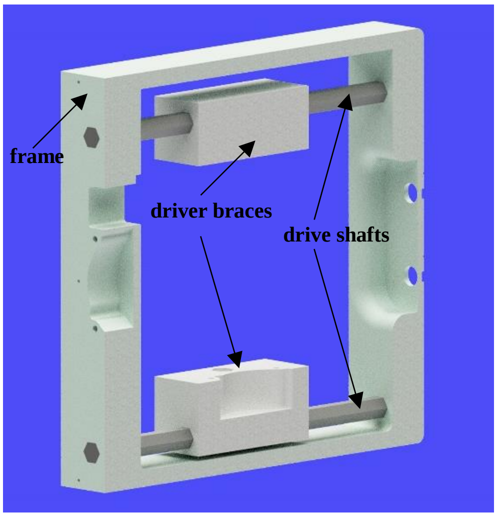

Figure 11: Section View of frame with driver braces the drive shafts

Additionally, an X-stage encoder system is assembled to enhance the accuracy of the current motion. The encoder system includes the encoder, the encoder strip (LIN-500-4-1, US Digital Corporation, Vancouver, Washington, USA), the strip holder and the strip supporter. Tthe Figure 12 shows, the encoder as it is located on the upper surface of the upper X-stage driver brace. The encoder strip is secured between the strip holder and the strip supporter. The strip supporter is rigidly joined to the upper surface of the frame. While the X-stage produce its desired motion, the driver brace , thus the encoder, move along the encoder strip. Due to this, the detection of the robotic system's lateral movement is provided and the accuracy of the current motion is ensured.

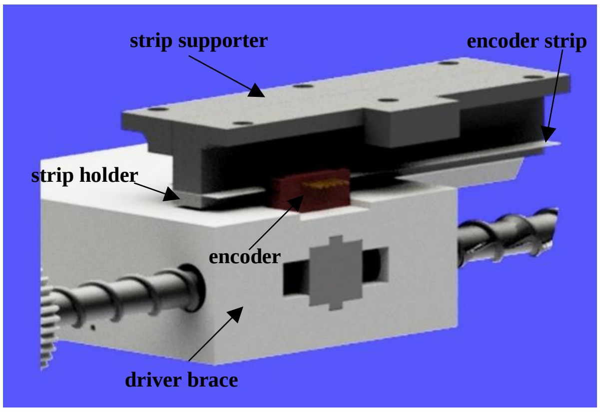

Figure 12: X-stage encoder system with driver brace

Figure 13A illustrates the board 1 which is rigidly placed on the side of the frame as shown in Figure 14A. Figure 13B shows the board 2 which is securely positioned between the boards 1 and 3. The board 3 is presented in Figure 13C and is used aims to protect the retainers.

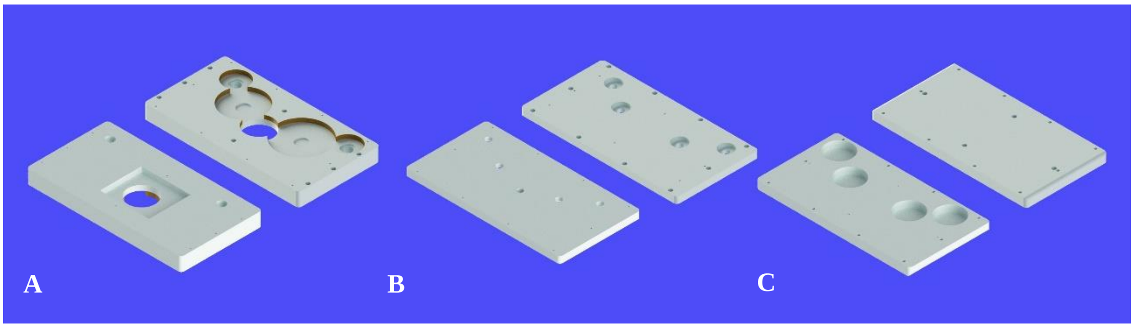

Figure 13: (A) Board 1 (B) Board 2 (C) Board 3

The retainers and the spindles are used to enhance the secureness of the gears in regards to their undesirable lateral displacement that may occurs throughout their rotation. Additionally, this is achieved due to the insertion of the boards 1 and 2. As the Figure 14A shows, the board 1 has been constructed to create a shell, considered as gears' case, to which the gears are going to be placed. Two spindles are coincentrically fixed on the previously mentioned gears. The spindles and the jack screws penetrate the created holes of the board 2 which is coupled to the board 1. The board 2 functions as the gears' cover and as the retainers' base. The retainers are placed on the other side of the board allowing their rotation as shown in Figure 14B. It is important to note that the retainers that are located at the pinions are coupling to the jack screws, whilst the two rest retainers are coupled with the two spindles. Due to the coupling between the retainers and the screws, the screws' stability is enhanced.

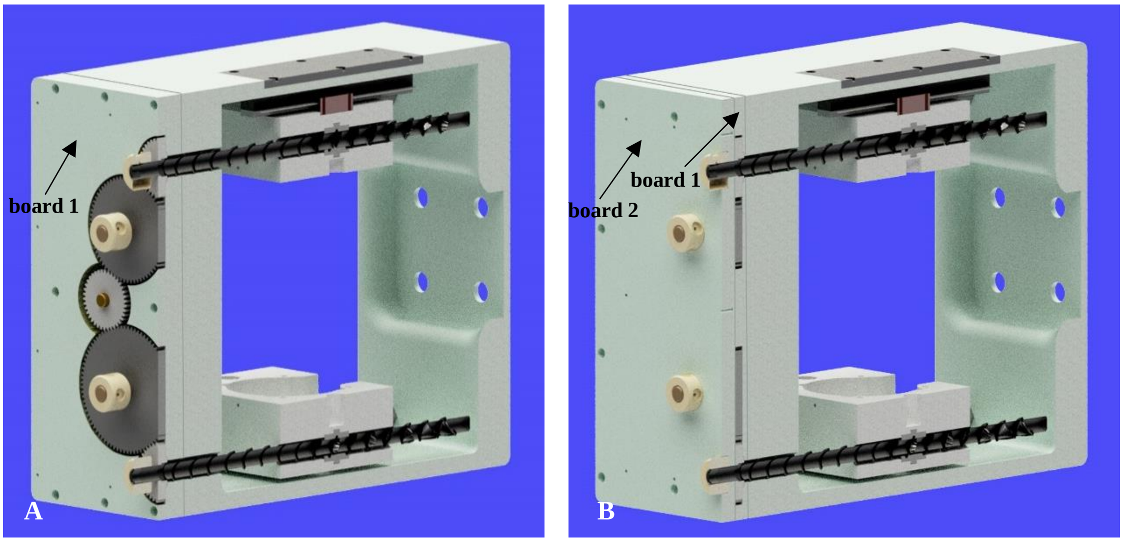

Figure 14: (A) Board 1 coupled to frame (B) Board 2 coupled to frame

After the implementation of the boards 1 and 2, the board 3 has been constructed to protect and enclose the retainers (Figure 15).

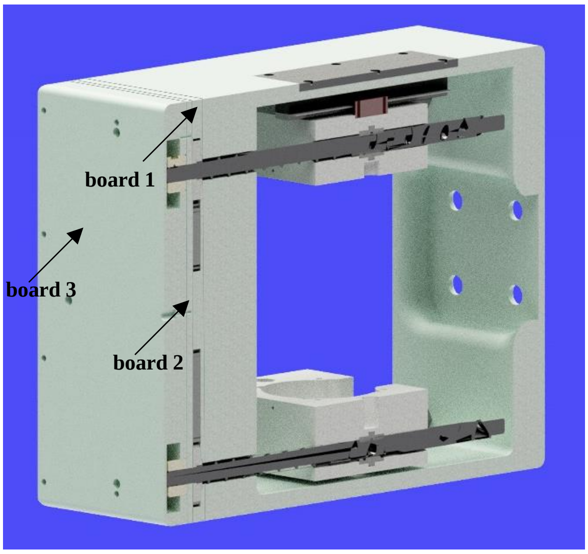

Figure 15: Board 3 coupled to frame

Conclusively, the entire motion system of the developed robotic positioning device is presented in Figure 16. Figure 16A illustrates the combination of the two motion stages (X-stage and Y-stage) that construct the entire biopsy system. As it is shown, a vertical oriented board, considered as the horizontal driver braces' stabilizer is added in the robotic system. The development of the current part aims to enhance the stability between the two driver braces that are included in the X-stage. To achieve this the board is joined to the side surfaces of both driver braces. It is also used to prevent any undesired lateral movement and ensure the simultaneous displacement of the X-stage's driver braces.

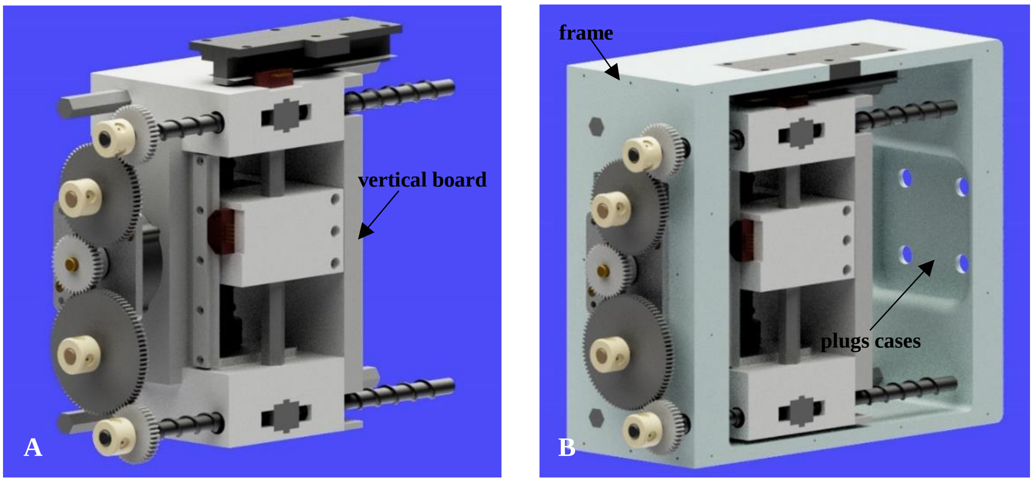

Figure 16: (A) Robotic system's entire mechanical system (B) Robotic system's entire mechanical system with frame

Figure 16B shows the entire motion system of the constructed positioning device enclosed in the frame part. The frame has been developed with holes, called as plugs cases, on its side where the plugs of the motors and encoders are fixed. Moreover, as it has been already mentioned, one of the frame's main functions is to enclose the mechanical part of the robotic system. For the same purpose, the covers are assembled. These covers are respectively coupled to the front and back side of the frame. Figure 17 shows, an orthogonal empty gap has been constructed to both covers. This empty area is developed to provide to the user of the robotic device the capability to access the Y-stage's driver brace, as shown in Figure 18. The driver brace must be accessible to insert the syringe, the needle supporter and the biopsy needle inside its constructed spaces.

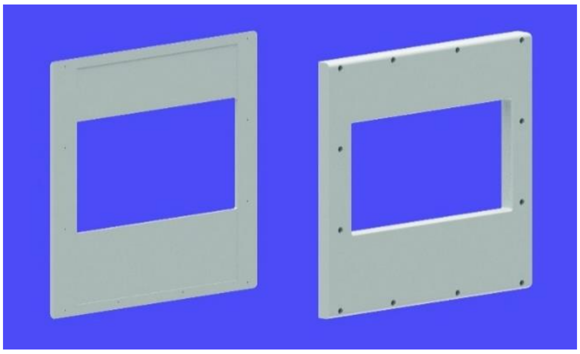
Figure 17: Back cover (left) and Front cover (right

Figure 18: Front and back cover coupled on frame

Conclusions

The above description is about an MR compatible robotic system which aims to place on the desired location a biopsy needle, to complete a breast biopsy procedure. Specifically, the robotic device's purpose is to move the biopsy needle supporter to which a biopsy needle is inserted to target a breast tumor.

Moreover, as it has been explained earlier, the robotic system contains to stages of motion; the X-stage and the Y-stage. The X-stage and the Y-stage are individually operated to move the needle supporter along the x-axis and the y-axis, respectively. However, few calculations are occurred to estimate the range of motion that each of the motion stages is capable to provide. Characteristically, the X-stage efficiently provides a maximum horizontal displacement (x-axis) equal to 9.00 cm approximately. Likewise, the Y-stage produces a vertical motion that is capable to move the needle supporter at a maximum distance equal to 13.00 cm approximately. Therefore, the area considering as a procedure area that the robotic system provides to the user (doctor) to operate the breast biopsy is 117.00 cm^2.

Furthermore, the materials provide to the robotic system's parts the required MR compatibility. In the same manner, the electromechanical components that both X-stage and Y-stage include MR compatible. In addition to this, due to the location of the motors and the encoders the MRI scanner's operation remains unaffected.

The construction design has been illustrated considering the requirement that the developed robotic system must be positioned on the MRI scanner's bed. Regarding the construction design, it is also important to note that the frame and the covers protect the electromechanical system of the positioning device. Except for this, the enclosure of the electromechanical system results to the easier and more secure transportation of the developed device. Thus, the MRBREASTBIO becomes a universal and portable device which fits in all the available MRI scanners.

As a final point, the positioning device includes piezoelectric motors, MR compatible encoders, PLA plastic and ASA plastic, fisher connectors and brass screws. The proposed system can be easily reduced in size if this is required for some other applications.

References

[1] World Health Organization (WHO), “Breast Cancer. Source: Globocan 2020.” [Online]. Available: https://gco.iarc.fr/today/data/factsheets/cancers/20-Breast-fact-sheet.pdf. [Accessed: 11-Oct-2022].

[2] Z. Momenimovahed and H. Salehiniya, “Epidemiological characteristics of and risk factors for breast cancer in the world,” *Breast Cancer Targets Ther.*, vol. 11, pp. 151–164, 2019, doi: 10.2147/BCTT.S176070.

[3] S. K. Patterson, “Image-guided percutaneous breast biopsies,” *Imaging Med.*, vol. 3, no. 5, pp. 597–605, 2011, doi: 10.2217/iim.11.42.

[4] T. H. Helbich, W. Matzek, and M. H. Fuchsjäger, “Stereotactic and ultrasound-guided breast biopsy,” *Eur. Radiol.*, vol. 14, no. 3, pp. 383–393, 2004, doi: 10.1007/s00330-003-2141-z.

[5] G. Schueller, C. Schueller-Weidekamm, and T. H. Helbich, “Accuracy of ultrasound-guided, large-core needle breast biopsy,” *Eur. Radiol.*, vol. 18, no. 9, pp. 1761–1773, 2008, doi: 10.1007/s00330-008-0955-4.

[6] C. M. Sommerich *et al.*, “Collaborating with cardiac sonographers to develop work-related musculoskeletal disorder interventions,” *Ergonomics*, vol. 59, no. 9, pp. 1193–1204, 2016, doi: 10.1080/00140139.2015.1116613.Collaborating.

[7] A. M. Priester, S. Natarajan, and M. Culjat, “Robotic ultrasound systems in medicine,” *IEEE Trans. Ultrason. Ferroelectr. Freq. Control*, vol. 60, no. 3, pp. 507–523, 2013, doi: 10.1109/TUFFC.2013.2593.

[8] G. Megali *et al.*, “A computer-assisted robotic ultrasound-guided biopsy system for video-assisted surgery,” *Lect. Notes Comput. Sci. (including Subser. Lect. Notes Artif. Intell. Lect. Notes Bioinformatics)*, vol. 2208, pp. 343–350, 2001, doi: 10.1007/3-540-45468-3_41.

[9] V. G. Mallapragada, N. Sarkar, and T. K. Podder, “Robot-assisted real-time tumor manipulation for breast biopsy,” *IEEE Trans. Robot.*, vol. 25, no. 2, pp. 316–324, 2009, doi: 10.1109/TRO.2008.2011418.

[10] V. Mallapragada, N. Sarkar, and T. K. Podder, “Toward a robot-assisted breast intervention system,” *IEEE/ASME Trans. Mechatronics*, vol. 16, no. 6, pp. 1011–1020, 2011, doi: 10.1109/TMECH.2010.2068575.

[11] N. Bluvol, A. Sheikh, A. Kornecki, D. Del Rey Fernandez, D. Downey, and A. Fenster, “A needle guidance system for biopsy and therapy using two-dimensional ultrasound,” *Med. Phys.*, vol. 35, no. 2, pp. 617–628, 2008, doi: 10.1118/1.2829871.

[12] W. L. Smith, K. J. M. Surry, G. R. Mills, D. B. Downey, and A. Fenster, “Three-Dimensional Ultrasound-Guided Core Needle Breast Biopsy,” *Ultrasound Med. Biol.*, vol. 27, no. 8, pp. 1025–1034, 2001.

[13] T. R. Nelson, A. Tran, H. Fakourfar, and J. Nebeker, “Positional calibration of an ultrasound image-guided robotic breast biopsy system,” *J. Ultrasound Med.*, vol. 31, no. 3, pp. 351–359, 2012, doi: 10.7863/jum.2012.31.3.351.

[14] M. Abayazid, P. Moreira, N. Shahriari, S. Patil, R. Alterovitz, and S. Misra, “Ultrasound-guided three-dimensional needle steering in biological tissue with curved surfaces,” *Med. Eng. Phys.*, vol. 37, no. 1, pp. 145–150, 2015, doi:

10.1016/j.medengphy.2014.10.005.

[15] M. K. Welleweerd, F. J. Siepel, V. Groenhuis, J. Veltman, and S. Stramigioli, "Design of an end-effector for robot-assisted ultrasound-guided breast biopsies," *Int. J. Comput. Assist. Radiol. Surg.*, vol. 15, no. 4, pp. 681–690, 2020, doi: 10.1007/s11548-020-02122-1.

[16] M. Michell, *Breast Cancer*, 1st ed. Cambridge University Press, 2010.

[17] "Affirm Breast Biopsy Guidance System." Hologic. https://www.hologic.com/hologic-products/breast-health-solutions/affirm-breast-biopsy-guidance-system. Accessed: 25/10/2022

[18] "Affirm Prone Breast Biopsy System." Hologic. https://www.affirmpronebiopsy.com/ Accessed: 25/10/2022

[19] K. J. M. Surry, G. R. Mills, K. Bevan, D. B. Downey, and A. Fenster, "Stereotactic mammography imaging combined with 3D US imaging for image guided breast biopsy," *Med. Phys.*, vol. 34, no. 11, pp. 4348–4358, 2007, doi: 10.1118/1.2794175.

[20] K. J. M. Surry, W. L. Smith, L. J. Campbell, G. R. Mills, D. B. Downey, and A. Fenster, "The development and evaluation of a three-dimensional ultrasound-guided breast biopsy apparatus," *Med. Image Anal.*, vol. 6, pp. 301–312, 2002.

[21] A. Fenster, K. J. M. Surry, G. R. Mills, and D. B. Downney, "3D ultrasound guided breast biopsy system," *Ultrasonics*, vol. 42, pp. 769–774, 2004, doi: 10.1016/j.ultras.2003.11.004.

[22] D. Saslow *et al.*, "American Cancer Society Guidelines for Breast Screening with MRI as an Adjunct to Mammography," *CA Cancer J Clin*, vol. 57, no. 2, pp. 75–89, 2007.

[23] L. L. LaTrenta LR, Menell JH, Morris EA, Abramson AF, Dershaw DD, "Breast lesions detected with MR imaging: utility and histopathologic importance of identification with US," *Radiology*, vol. 227, no. 3, pp. 856–861, 2003, doi: 10.1148/radiol.2273012210.

[24] C. D. Lehman, E. R. DePeri, S. Peacock, M. D. McDonough, W. B. DeMartini, and J. Shook, "Clinical experience with MRI-guided vacuum-assisted breast biopsy," *Am. J. Roentgenol.*, vol. 184, no. 6, pp. 1782–1787, 2005, doi: 10.2214/ajr.184.6.01841782.

[25] T. Perretta, C. A. Pistolese, F. Bolacchi, E. Cossu, V. Fiaschetti, and G. Simonetti, "Imaging RM. Biopsia della mammella con sistema di retro aspirazione RM guidato da 10 gauge: Caratterizzazione istologica," *Radiol. Medica*, vol. 113, no. 6, pp. 830–840, 2008, doi: 10.1007/s11547-008-0289-y.

[26] R. Plantade and I. Thomassin-Naggara, "MRI vacuum-assisted breast biopsies," *Diagn. Interv. Imaging*, vol. 95, no. 9, pp. 779–801, 2014, doi: 10.1016/j.diii.2013.12.023.

[27] R. H. El Khouli *et al.*, "MRI-Guided Vacuum-Assisted Breast Biopsy : A Phantom and Patient Evaluation of Targeting Accuracy," *J. Magn. Reson. Imaging*, vol. 429, pp. 424–429, 2009, doi: 10.1002/jmri.21831.

[28] S. H. Heywang-Köbrunner, R. Sinnatamby, A. Lebeau, A. Lebrecht, P. D. Britton, and I. Schreer, "Interdisciplinary consensus on the uses and technique of MR-guided vacuum-assisted breast biopsy (VAB): Results of a European consensus meeting," *Eur. J. Radiol.*, vol. 72, no. 2, pp. 289–294, 2009, doi: 10.1016/j.ejrad.2008.07.010.

[29] E. C. Gombos *et al.*, "MR guided breast interventions: role in biopsy targeting and lumpectomies," *Magn Reson Imaging Clin N Am.*, vol. 23, no. 4, pp. 547–561, 2016, doi: 10.1016/j.mric.2015.05.004.MR.

[30] M. C. Chevrier, J. David, M. El Khoury, L. Lalonde, M. Labelle, and I. Trop, “Breast Biopsies Under Magnetic Resonance Imaging Guidance: Challenges of an Essential but Imperfect Technique,” *Curr. Probl. Diagn. Radiol.*, vol. 45, no. 3, pp. 193–204, 2016, doi: 10.1067/j.cpradiol.2015.07.002.

[31] W. Kaiser, H. Fischer, J. Vagner, and M. Selig, “Robotic System for Biopsy and Therapy of Breast Lesions in a High-Field Whole-Body Magnetic Resonance Tomography Unit,” *Invest. Radiol.*, vol. 35, no. 8, pp. 513–519, 2000.

[32] B. T. Larson, A. G. Erdman, N. V. Tsekos, E. Yacoub, P. V. Tsekos, and I. G. Koutlas, “Design of an MRI-Compatible Robotic Stereotactic Device for Minimally Invasive Interventions in the Breast.,” *J Biomech Eng.*, vol. 126, no. 4, pp. 458–465, 2004.

[33] R. Kokes *et al.*, “Towards a Teleoperated Needle Driver Robot with Haptic Feedback for RFA of Breast Tumors under Continuous MRI,” *Med Image Anal.*, vol. 13, no. 3, pp. 445–455, 2009, doi: 10.1016/j.media.2009.02.001.

[34] B. Yang *et al.*, “Design , development , and evaluation of a master – slave surgical system for breast biopsy under continuous MRI,” *Int. J. Rob. Res.*, vol. 33, no. 4, pp. 616–630, 2014, doi: 10.1177/0278364913500365.

[35] K. G. Chan, T. Fielding, and M. Anvari, “An image-guided automated robot for MRI breast biopsy,” *Int. J. Med. Robot. Comput. Assist. Surg.*, vol. 12, no. 3, pp. 461–477, 2016, doi: 10.1002/rcs.

[36] S. Byeongjun, P. J. Kim, K. L. C. Yoon, and D. K. H. K. Y. Jo, “A magnetic resonance image-guided breast needle intervention robot system : overview and design considerations,” *Int. J. Comput. Assist. Radiol. Surg.*, vol. 12, no. 8, pp. 1319–1331, 2017, doi: 10.1007/s11548-017-1528-2.

[37] V. Groenhuis, F. J. Siepel, J. Veltman, J. K. van Zandwijk, and S. Stramigioli, “Stormram 4: An MR Safe Robotic System for Breast Biopsy,” *Ann. Biomed. Eng.*, vol. 46, no. 10, pp. 1686–1696, 2018, doi: 10.1007/s10439-018-2051-5.

[38] V. Groenhuis, J. Veltman, and S. Stramigioli, “Stormram 2: A MRI-compatible robotic system for breast biopsy,” in *Proceedings of The Hamlyn Symposium on Medical Robotics*, 2016, pp. 52–53.

[39] V. Groenhuis, J. Veltman, J. Siepel, and S. Stramigioli, “Stormram 3: A Magnetic Resonance Imaging-Compatible Robotic System for Breast Biopsy,” in *Special Issue on Surgical Robot Challenge*, 2017, pp. 34–41.

[40] T. Zhang, D. Navarro-alarcon, K. W. Ng, M. K. Chow, Y. Liu, and H. L. Chung, “A Novel Palm-Shape Breast Deformation Robot for MRI-Guided Biopsy A Novel Palm-Shape Breast Deformation Robot for MRI-Guided Biopsy,” in *2016 IEEE International Conference on Robotics and Biomimetics (ROBIO)*, 2016, pp. 527–532, doi: 10.1109/ROBIO.2016.7866376.